JOURNAL OF COMPUTATIONAL PHYSICS **146,** 707–725 (1998)
ARTICLE NO. CP986080

On Numerical Approximation of Electrostatic Energy in 3D

Daniele Finocchiaro,* Marco Pellegrini,†,[1] and Paolo Bientinesi‡

*Scuola Normale Superiore, Pisa, Italy; †Institute for Computational Mathematics of CNR, Pisa, Italy; ‡University of Pisa, Pisa, Italy
E-mail: fino@cibs.sns.it, pellegrini@imc.pi.cnr.it, bientin@matcomp1.imc.pi.cnr.it

Received February 12, 1998; revised August 4, 1998

Approximating the Coulomb self-energy of a charge distribution within a three-dimensional domain and the mutual Coulomb energy of two charge distributions often constitutes a computational bottleneck in the simulation of physical systems. The present article reports on a recently developed computational technique aimed at the numerical evaluation of the six-dimensional integrals arising from Coulomb interactions. Techniques from integral geometry are used to show a reduction of the domain from six-dimensional to two-dimensional. In the process analytic singularities due to Coulomb's law are eliminated. Experimental results on the self-energy of a charged cube show that the proposed method converges rapidly and is competitive with methods proposed in the literature for similar integration problems.

1. INTRODUCTION

1.1. *The Problem*

Suppose we are given a domain $D \subseteq R^3$ in 3-space and a volume charge density function ρ defined in D; the electrostatic or Coulomb self-energy of D using the Gaussian unit system is given by the following six-dimensional integral:

$$E_D = \frac{1}{2} \int_{p_1, p_2 \in D} \frac{\rho(p_1)\rho(p_2)}{|p_1 - p_2|}\, dp_1\, dp_2. \tag{1}$$

If we are given two domains, D_1 and D_2, in 3-space, endowed respectively with volume charge density functions ρ_1 and ρ_2, the mutual Coulomb energy is given by the following

[1] Corresponding author.

0021-9991/98 $25.00

six-dimensional integral:

$$E_{D_1,D_2} = \int_{p_1 \in D_1} \int_{p_2 \in D_2} \frac{\rho_1(p_1)\rho_2(p_2)}{|p_1 - p_2|}\, dp_1\, dp_2. \tag{2}$$

Integrals of this form are found often in physics and chemistry but rarely are closed-form solutions known (however, a notable exception is reported in the next subsection). Numerical evaluation of integrals (1) and (2) encounters two sources of inefficiency. First of all these integrals are six-dimensional, thus requiring a large number of cubature points. As a rule of thumb, the approximation achieved with n quadrature points in dimension 1, is reached with n^6 cubature points in dimension 6, when product quadrature rules are used. Second, the integrand function has a singularity whenever the two points p_1 and p_2 coincide, which happens in integral (1) and may happen in integral (2), as we do not rule out domains that share boundary points. The presence of singularities induces slow convergence in standard numerical integration methods.

In this paper we show that for a vast class of domains and density functions it is possible to transform integrals (1) and (2) so that the kernel is regular and the dimension of the integration domain is reduced to 2, thus making numerical integration an appealing option. Before we say more about our results we comment on two application areas where such results may be beneficial.

1.2. *Applications*

1.2.1. Molecular computations. The well-known electron–electron repulsion integral (ERI) is

$$(\phi_\mu \phi_\nu \,|\, \phi_\lambda \phi_\sigma) = \int_{p_1,\, p_2 \in R^3} \frac{\phi_\mu(p_1)\phi_\nu(p_1)\phi_\lambda(p_2)\phi_\sigma(p_2)}{|p_1 - p_2|}\, dp_1\, dp_2, \tag{3}$$

where ϕ_μ, ϕ_ν, ϕ_λ, and ϕ_σ are one-electron orbitals. Such integrals are found in many *ab initio* theories and methods, Hartree–Fock theory and density-functional theory [1, 2], to mention a couple of the most important ones. The ERI has the same mathematical structure of the energy integral (2) when we consider as domains D_1 and D_2 the whole space and we interpret $\phi_\mu\phi_\nu$ (resp. $\phi_\lambda\phi_\sigma$) as the function associated with the first (resp. second) domain.

One-electron basis functions are then usually expanded as a linear combination of primitive basis functions. Gaussian type functions [3] have become one of the most popular choices for the basis expansion of atomic orbitals since the pioneering work of Boys [4] showing that the ERI, as well as other relevant integrals, have an analytic exact solution for such a class of functions. These analytic solutions are usually obtained through the evaluation of recursive schemes [5–7], or through the so-called Rys polynomial technique [8–10].

Boerrigter, te Velde, and Bearends [11] note that a large number of Gaussian-type functions might be needed to tightly approximate one-electron orbitals, thus making the rapid growth of the number of integrals to be evaluated a particularly vexing problem. Other types of basis functions (e.g., Slater-type orbitals, plane weaves, Bessel functions) may lead to shorter expansions, but suffer from the difficulty of analytic or numerical integration. In [11, 12] a cellular approach is used: the space is partitioned in Voronoi polyhedra, where

a Voronoi polyhedron is the portion of space closer to a nucleus than any other. Then each polyhedron is split into an inner sphere centered on the atom center and a set of truncated pyramids. Specialized numerical techniques are then used in these two types of domains. Numerical results reported in [11] compare favorably with previously known techniques, notably those based on Diophantine integration [13, 14]. Such a method is suitable for computing particle-distribution interaction integrals, since special attention is paid to singularities at the nuclei; however, such a technique does not seem to address more general (six-dimensional) integrals (1) and (2).

A second numerical technique is advocated by Becke [15] (see also [16–18]). In [16] integral (3) is split into an external part, corresponding to integration in dp_2, and an internal part, corresponding to integration in dp_1 for a fixed p_2. The internal integral is the potential of the charge distribution $\phi_\mu\phi_\nu$ at the fixed point p_2. Such a potential is calculated by considering the equivalent Poisson equation and a finite-difference solution approach. The external integral is then attacked with a technique in [15]. Starting from Voronoi cells based on atomic nuclei Becke defines suitable weighting functions that are continuous, close to the unity within a Voronoi cell, and close to zero outside. Using these weight functions, an arbitrary three-dimensional integral can be reduced to a sum of atom-centered integrals, for which product quadrature rules in spherical coordinates are used.

Further refinements and tuning of the approaches in [11, 15] for three-dimensional integrals are investigated in [19]. The approach in [20, 21] to the evaluation of integrals of potential theory has some high level similarity with that of Becke, although in a different context.

1.2.2. Energy calculations for crystals. In several models of matter we can distinguish a discrete component made of charged point particles and a continuous component made of continuous distributions of charge (see, e.g., [22]). Thus formally we can split the total electrostatic energy into the contribution of the point charges, the mutual energy due to the interaction of point charges with the distribution of charge, and finally, the contribution of the distribution of charge. The first contribution is expressed formally as a double summation of the Coulomb energy over pairs of particles. Several techniques, ranging from fast n-body methods to periodic boundary conditions (Madelung sums [23], Ewald summation [24]), are available to speed up the computation. The second contribution involves a sum of three-dimensional integrals. Numerical techniques for such integrals have been mentioned above in the context of DFT calculations. In the special case of uniform distribution in a cube some analytic solutions are also known [25, 26]. For the energy of distribution of charges, which are represented by six-dimensional integrals of type (1) or (2), save the above-mentioned references, there is a notable lack of specific techniques available.

In the study of crystal or quasicrystal lattices it is customary to associate each particle with a convex polyhedron containing the particle. Besides Voronoi cells, space filling polyhedra are also used [27, 28]. Moreover, we may want to associate a charge distribution to each polyhedron (e.g., to maintain electroneutrality). Although a constant distribution of charge is a reasonable first choice, more precise models might include nonconstant distributions to fit known data (either experimental or obtained through auxiliary computations). Thus, energy calculations for regular crystal lattices (not necessarily with cubic symmetry), or even irregular lattices, do conceivably benefit from general techniques for computing six-dimensional energy integrals over convex polyhedral domains with nonconstant densities of charge.

1.3. *Main Results, Experiments, and Comparisons*

The main contribution of this paper is a general efficient method to compute integrals (1) and (2) when:

- The domain D (resp. D_1 and D_2) is a compact convex polyhedron.
- The density ρ (resp. ρ_1 and ρ_2) is a polynomial function in Cartesian coordinates.

As we noted above convex polyhedral domains arise naturally in methods based on Voronoi tassellations or on space-filling polyhedra. Although most popular basis functions are not polynomial (usually exponential terms are present), piecewise polynomial functions may be used to fit any given function in three-dimensional space.

The proposed method has been implemented and tested on approximating the self-energy of a uniformly charged cube (a more detailed description is in Section 5). A reference value is obtained by a high-order Gaussian integration of the formula in [26] for the potential of a cube at a point. As a focus for comparison we concentrate on the following experimental result: using 1000 Gaussian points our method attains an absolute error between 10^{-5} and 10^{-6}, without exploiting the symmetries of the cube. If we exploit explicitly symmetries of the cube for the same number of points the absolute error of our method is in the range between 10^{-9} and 10^{-10}.

In [11, p. 103] an accuracy of 10^{-3} using a number of points per polyhedron in the range from 700 (for hydrogen) to 3000 (for uranium), and exploiting symmetries is reported. However, the integrals considered in [11] are three-dimensional while ours are six-dimensional before the geometric transformation. Results in [12, pp. 95–96] on computing the overlap integrals (three-dimensional) for a Slater-type function in a convex polyhedron show an error in the range $[10^{-6}, 10^{-7}]$ for a number of points from 2500 for small molecules with many symmetries up to 264,000 for large molecules without symmetries.

In [15] precision in the range from 10^{-4} to 10^{-5} is reported using a grid of integration points of size equal to or greater than $20 \times 50 \times 50 = 50{,}000$ for the integration of three-dimensional[2] functions whose analytic closed form is known.

Our preliminary experiments and comparisons with results in [11, 12, 15] indicate that our method for six-dimensional integrals can attain performances comparable to those of competing methods even when applied just to three-dimensional integrals.

1.4. *Integral Geometry and Computational Geometry*

Our result is obtained by applying to integrals (1) and (2) geometric transformations already applied successfully to other problems ranging from radiosity (approximation of form factors [29]), to calculation of electrostatic forces [30] and the boundary element method (entries of the stiffness matrix for systems of conducting bodies [31, 32]).

The first step of the transformation involves transforming integrals (1) and (2) into integrals over lines in 3-space. The second step consists in choosing a particular form of the differential measure of lines in 3-space so that we can separate our integral into an external integral over the set of directions and an internal integral which can be evaluated analytically. The new kernel is evaluated using methods from computational geometry. As a result the initial six-dimensional integral is reduced to a two-dimensional one. Moreover, while the original kernel in (1), (2), and (3) is singular, the new kernel is regular everywhere in the

[2] Such integrals are expressed in spherical coordinates, thus with a linear and two angular parameters.

domain of integration. Although the general scheme is the same as in the above-mentioned results, the transformation depends critically on the exponent of the factor $|p_1 - p_2|$, thus requiring in this paper a new derivation starting from first principles.

1.5. *Organization of the Paper*

The paper is organized as follows. In Section 2 we give the geometric transformation of integrals (1) and (2) for any convex compact polyhedron endowed with a *uniform* charge density. In Section 3 the result is extended to any distribution of charge polynomial in Cartesian coordinates. In Section 4 we describe the overall algorithm. In Section 5 we discuss the implementation, experiments, and numerical results.

2. GEOMETRIC TRANSFORMATION: UNIFORM CHARGE DENSITY

In this section we assume that the domain D of interest is a convex and compact body B in three-dimensional space, endowed with a *uniform* charge density ρ. We assume the space to be vacuous or filled with a homogeneous nonpolarizable medium, and we assume a fixed coordinate system. The purpose of this section is to use tools from integral geometry and differential calculus in order to rewrite Eqs. (1) and (2) in a form convenient for numerical integration. We begin by considering the electrostatic potential generated by the body B at a point p of the space:

$$V_B(p) = \rho \int_{q \in B} \frac{1}{|p - q|}\, dq. \tag{4}$$

The idea is to express $V_B(p)$ as a weighted integral over the set of straight lines passing through p. The weight of each line L is given by the charges lying on L, and it can be expressed in terms of the length of the intersection of L with the body B.

2.1. *Preliminaries*

Let us introduce some notation, as well as recall some elements of differential calculus and integral geometry (see, e.g., [33, 34]). The first step is to introduce the set of straight lines in space and define a measure on it. We denote with $\mathcal{L}$ the set of straight lines in three-dimensional space. Given a point p, $\mathcal{L}_p$ is the set of lines $L \in \mathcal{L}$ passing through p. We will use L for lines in either $\mathcal{L}$ or $\mathcal{L}_p$, but to make the expressions clearer we will denote their differential measures of lines respectively with dL and dL_p. A straight line can be identified in a number of different ways, depending on the coordinates used. To determine a line in $L \in \mathcal{L}_p$ we only need to specify a direction u, so that $L \equiv L(u)$. For a generic line $L \in \mathcal{L}$, for reasons that will become apparent soon, we specify a direction u and the intersection s between L and a plane S_u orthogonal to u, so that $L \equiv L(s, u)$. Note that this is just one particular parameterization of lines in the space.

Santaló [34] explains how to find a density for subsets of $\mathcal{L}$ which is invariant under the group of rigid motions; moreover, this density is unique up to a constant factor. The density for straight lines in the space is simply

$$dL = ds\, du,$$

where du is the differential measure of directions and ds is the surface element on a plane

S_u normal to u. This nice relation justifies our choice of (s, u) to determine L. Other representation of lines produce more complicated expressions.

The direction u corresponds to a point on the surface of a unit sphere. However, it will be convenient to identify antipodal points, so that we will really be working on a hemisphere denoted with $\frac{1}{2}\Omega$ whose measure is thus 2π. If we express the direction u in polar coordinates (θ, ϕ) then it holds $du = \sin\theta \, d\phi \, d\theta$. For the set $\mathcal{L}_p$ we have simply $dL_p = du$. Intuitively, this differential element can be seen as a small cone with vertex p, extending in both directions from p, where du equals the solid angle at p. The measure of the entire set $\mathcal{L}_p$ is $\int dL_p = |\frac{1}{2}\Omega| = 2\pi$. The physical dimension of dL is $[\mathtt{length}^2]$, while dL_p is adimensional.

Now we relate these differential elements to the element of volume $dq = dx\, dy\, dz$ at the point q of a body B. In fact this will enable us to rewrite in a more geometric fashion the classical potential formula. Fix a point p, and let $r = |p - q|$ be the distance between q and p; then it holds that

$$dq = r^2 \, dr \, dL_p. \tag{5}$$

This can be obtained by using polar coordinates, writing $x = r\sin\theta\cos\phi$, $y = r\sin\theta\sin\phi$, $z = r\cos\phi$, and applying the rules of exterior calculus. It is also easily seen geometrically because dq is approximated by a cylinder with base $r^2\, dL_p$ and height dr [33].

The other important relation that we need relates the (exterior) product of two differential volumes to the differential of lines. Let L be the line passing through points p and q, and let r_1 (resp. r_2) be the distance of p (resp. q) from a fixed point of reference on L. The following holds [34, p. 237]:

$$dp\, dq = |r_1 - r_2|^2 \, dL \, dr_1 \, dr_2. \tag{6}$$

2.2. *Electrostatic Potential at a Point*

We are now ready to find a formula alternative to (4) for the potential field generated by a convex body B with uniform charge density. The intuition behind the following theorem is that we take a differential cone with vertex p and sum up the contributions of all the charges lying in the cone. We find their total contribution to be $(r_{\max}^2 - r_{\min}^2)\, dL_p$. Next we integrate over all the directions L_p. The effect due to a fixed differential charge is counted exactly once, because there is only one line $L \in \mathcal{L}_p$ passing through it.

THEOREM 1. *For a line $L \in \mathcal{L}_p$, let $\ell = |L \cap B|$ and $m = |L \cap C|$, where C is the convex hull of B and p. Then the potential $V_B(p)$ generated by B at a point p external to B is*

$$V_B(p) = \frac{\rho}{2} \int_{L \cap B \neq \emptyset} \ell(2m - \ell) \, dL_p, \tag{7}$$

where the integral is over the set $\mathcal{L}_p$. If p is inside B, the potential at p is

$$V_B(p) = \frac{\rho}{2} \int_{\mathcal{L}_p} \left(\ell_1^2 + \ell_2^2\right) dL_p, \tag{8}$$

where ℓ_1 and ℓ_2 are the lengths of the two segments in which p splits $L \cap B$.

Proof. Let p be external to B, and fix a line L through p and intersecting B. Clearly $p \notin L \cap B$. We denote with $r_{\min}$ and $r_{\max}$ the minimum and maximum distance of p from the points of $L \cap B$. Now the potential at p is given by the classical formula (4), which in view of (5) becomes

$$V_B(p) = \int_{q\in B} \frac{\rho}{|p-q|}\, dq = \rho \int_{L\in\mathcal{L}_p} \int_{q\in L\cap B} r\, dr\, dL_p,$$

where $r = |p-q|$. For a fixed line L intersecting B, we have $\int r\, dr = (r_{\max}^2 - r_{\min}^2)/2$ because r varies between values $r_{\min}$ and $r_{\max}$. If $L \cap B = \emptyset$ then $\int r\, dr = 0$. Consequently we can integrate on the domain $\{L \in \mathcal{L}_p : L \cap B \neq \emptyset\}$, thus obtaining

$$V_B(p) = \frac{\rho}{2} \int_{L\cap B\neq\emptyset} \left(r_{\max}^2 - r_{\min}^2\right) dL_p.$$

Now the first part of the theorem follows by substituting $\ell = r_{\max} - r_{\min}$ and $m = r_{\max}$ and rearranging the formula. This concludes the proof of the first part of the theorem.

When p is inside the body B, the previous reasoning applies to both directions of a single line L, where $r_{\min} = 0$ and $r_{\max} = l_1, l_2$, respectively. Moreover, all lines in $\mathcal{L}_p$ intersect B. This proves the second part of the theorem. ■

Formulas (7) and (8) have the important property of having a regular kernel, while in the classical formulation (4) the kernel may diverge.

2.3. *Self-Energy of a Body and Mutual Energy of Two Bodies*

Now we apply the result above in order to find the potential energy of a body or system of bodies. Intuitively, we will find that for a fixed differential element dL (which can be imagined as a "fat cone") the contribution to the total potential energy given by the interaction between charges in $B \cap dL$ is $\rho\ell^3 dL/6$. We will obtain the total energy by integrating all the differential contributions. The contribution of two fixed particular differential charges is counted exactly once, since two points define a unique straight line in the space.

THEOREM 2. *The potential self-energy E_B of a convex body B with uniform charge density ρ is given by*

$$E_B = \frac{\rho^2}{6} \int_{L\cap B\neq\emptyset} \ell^3\, dL, \tag{9}$$

where $L \in \mathcal{L}$ is a straight line in the space and ℓ is the length of the intersection $L \cap B$.

Proof. Let us start from the classical expression (1) for the potential energy of a body B, where ρ is constant and we use relation (6),

$$\begin{aligned} E_B &= \frac{\rho^2}{2} \int_{p,q\in B} \frac{1}{|p-q|}\, dp\, dq \\ &= \frac{\rho^2}{2} \int_{p,q\in B} |p-q|\, dL\, dr_1\, dr_2, \end{aligned}$$

where L is the line passing through p and q, and r_1, r_2 are the distances of p, q from a fixed point on L. We can exchange the order of integration, integrating first over the lines L

intersecting B and then over the pair of points laying on L. We obtain

$$E_B = \frac{\rho^2}{2} \int_{L \cap B \neq \emptyset} \left(\int_{p,q \in B \cap L} |p - q| \, dp \, dq \right) dL.$$

It can be easily seen that the inner integral evaluates to $\ell^3/3$, and the theorem follows. ■

The same result can be obtained starting from the well-known relation $E_B = (1/2) \int \rho(p) V_B(p) \, dp$ and applying formula (8) for the potential at a point.

The value $I_3 = \int \ell^3 \, dL$ is a geometric invariant of the object B, and the theorem we just proved is the three-dimensional case of a general relation which can be found in [34]. Using a formula from integral geometry [34, p. 231] we can obtain the bound $I_3 \leq (3/2)\mathcal{V}[B]\mathcal{A}[B]$ (where $\mathcal{V}[]$ and $\mathcal{A}[]$ denote respectively the volume and the superficial area), and this translates directly into a useful bound for E_B.

THEOREM 3. *The potential energy E_{B_1,B_2} of two convex bodies B_1, B_2, each with uniform charge density ρ_1, ρ_2, is given by*

$$E_{B_1,B_2} = \frac{\rho_1 \rho_2}{2} \int_{L \in \mathcal{L}_{12}} \ell_{B_1} \ell_{B_2} \left(2t - \ell_{B_1} - \ell_{B_2}\right) dL,$$

where $\ell_{B_1} = |L \cap B_1|$, $\ell_{B_2} = |L \cap B_2|$, $t = |L \cap C|$, C is the convex hull of B_1 and B_2, and $\mathcal{L}_{12}$ is the set of lines which intersect both B_1 and B_2.

Proof. We consider expression (2) and proceed like in the previous theorem. We obtain

$$E_{B_1,B_2} = \rho_1 \rho_2 \int_{\mathcal{L}_{12}} \left(\int_{p \in B_1 \cap L, q \in B_2 \cap L} |p - q| \, dp \, dq \right) dL.$$

By means of some calculus we obtain that the inner integral evaluates to $(1/2)\ell_{B_1}\ell_{B_2}(2t - \ell_{B_1} - \ell_{B_2})$ and the theorem follows. ■

3. GEOMETRIC TRANSFORMATION: NONUNIFORM DISTRIBUTION OF CHARGES

In this subsection we will extend the theory presented in Section 2 to the case of arbitrary distribution of charges. We will obtain formulas involving integrals over the set of straight lines, where each line is assigned a "weight" which depends on the body under study.

Consider first the electrostatic potential at a point p. For a generic distribution of charge on B formula (4) becomes

$$V_B(p) = \int_{q \in B} \frac{\rho(q)}{|p - q|} \, dq.$$

Proceeding like in the proof of Theorem 1 we can rewrite the last expression as

$$\begin{aligned} V_B(p) &= \int_{L \cap B \neq \emptyset} \int_{q \in L \cap B} \rho(q) r \, dr \, dL_p \\ &= \int_{L \cap B \neq \emptyset} w_{B,p}(L) \, dL_p, \end{aligned}$$

where we defined $w_{B,p}(L) = \int_{q \in L \cap B} \rho(q) r \, dr$. The quantity $w_{B,p}(L)$ can be thought of as the "weight" of line L and represents its contribution to the potential at p due to B. We already saw that $w_{B,p}(L)$ can be computed explicitly if $\rho(q)$ is constant. In the general case, we apply a change of coordinates as follows. Consider an orthogonal system of coordinates (x', y', z') which has the origin at p and the axis z' parallel to L. We rewrite the density function in this system of coordinates $\rho(p) \equiv \sigma(x', y', z')$. Notice that the coordinates x' and y' are the same for all the points on L, and we will write simply $\sigma(z') \equiv \sigma(x', y', z')$. The weight of line L is thus

$$w_{B,p}(L) = \int_{q \in L \cap B} \sigma(r) r \, dr.$$

Denoting with $\bar{\sigma}(x)$ an antiderivative of $\sigma(x)$, and with $\bar{\bar{\sigma}}(x)$ an antiderivative of $\bar{\sigma}(x)$, it is easily seen that $F(x) = \bar{\sigma}(x)x - \bar{\bar{\sigma}}(x)$ is an antiderivative of $\sigma(x)x$. Finally, let ℓ_1 and $\ell_2 \geq \ell_1$ be the z' coordinates of the extreme points of $L \cap \partial B$. We obtain for $w_{B,p}(L)$ the expressions

$$w_{B,p}(L) = \begin{cases} F(\ell_2) - F(\ell_1), & \text{if } p \notin B; \\ F(\ell_1) + F(\ell_2) - 2F(0), & \text{if } p \in B. \end{cases}$$

Consider now the self-energy of a body B, given by expression (1). In the same manner as before we obtain

$$\begin{aligned} E_B &= \int_{L \cap B \neq \emptyset} \int_{p,q \in L \cap B} \frac{1}{2} \rho(p) \rho(q) |p - q| \, dp \, dq \, dL \\ &= \int_{L \cap B \neq \emptyset} w_B(L) \, dL, \end{aligned} \tag{10}$$

where we defined

$$w_B(L) = \int_{p,q \in L \cap B} \frac{1}{2} \rho(p) \rho(q) |p - q| \, dp \, dq.$$

We can apply the same linear transformation as above to express $\rho(p)$ in a coordinate system (x', y', z'), where z' is parallel to L (the origin can be fixed arbitrarily). We denote the transformed function with $\sigma(x', y', z) \equiv \sigma(z')$, and define $\bar{\sigma}(x)$ and $\bar{\bar{\sigma}}(x)$ as before. Let ℓ_1 and $\ell_2 \geq \ell_1$ be the z' coordinates of the extreme points of $L \cap \partial B$. Then the weight of L can be written as

$$\begin{aligned} w_B(L) &= \int_{r_1, r_2 = \ell_1}^{\ell_2} \frac{1}{2} \sigma(r_1) \sigma(r_2) |r_1 - r_2| \, dr_1 \, dr_2 \\ &= \int_{r_1 = \ell_1}^{\ell_2} \sigma(r_1) [\bar{\bar{\sigma}}(r_1) - \bar{\sigma}(\ell_1)(r_1 - \ell_1) - \bar{\bar{\sigma}}(\ell_1)] \, dr_1 \qquad (11) \\ &= \bar{\sigma}(\ell_2) \bar{\bar{\sigma}}(\ell_2) + \bar{\sigma}(\ell_1) \bar{\bar{\sigma}}(\ell_2) - \bar{\bar{\sigma}}(\ell_1) \bar{\sigma}(\ell_2) - \bar{\sigma}(\ell_1) \bar{\bar{\sigma}}(\ell_1) \\ &\quad - \bar{\sigma}(\ell_1) \bar{\sigma}(\ell_2)(\ell_2 - \ell_1) - \int_{\ell_1}^{\ell_2} \bar{\sigma}(x)^2 \, dx. \qquad (12) \end{aligned}$$

It is an easy observation that for constant ρ this formula gives $w_B(L) = \rho^2 (\ell_2 - \ell_1)^3 / 6$, as we obtained in Theorem 2.

The case of two interacting bodies is in all similar to the one-body case, the only difference being in the integration limits for r_1 in expression (11).

4. ALGORITHM FOR THE EVALUATION OF THE INTEGRALS IN POLYHEDRAL DOMAINS

The formulas obtained so far for electrostatic quantities are not in a computable form because of the presence of the differential dL. In this subsection we will choose a particular parameterization of lines that is suitable for computation. We will obtain two-dimensional integrals with a smooth kernel. Moreover, we will explain how to compute this kernel exactly by analytic integration when the bodies are polyhedral objects and the charge distribution is polynomial in (x, y, z). To keep the discussion clear, we will focus our attention on the computation of E_B, given by formula (9) or its generalization (10).

As we explained in Subsection 2.1, we choose to represent a line L in 3-space as a pair (s, u), where $u \in \frac{1}{2}\Omega$ and $s \in S_u$. Denote with B_u the projection of the body B onto the plane S_u. A line $L \equiv (s, u)$ intersects B iff $s \in B_u$. So the energy of B in expression (10) can be written

$$E_B = \int_{u \in \frac{1}{2}\Omega} \int_{s \in B_u} w_B(s, u)\, ds\, du = \int_{\frac{1}{2}\Omega} K(u)\, du, \tag{13}$$

where

$$K(u) = \int_{s \in B_u} w_B(s, u)\, ds. \tag{14}$$

We integrate numerically over the set $\frac{1}{2}\Omega$ by approximating the integral with a weighted sum of values of the kernel $K(u)$ at selected points in the integration domain. The domain $\frac{1}{2}\Omega$ is a suitable domain of integration because a number of results exist on generating distributions of points on the sphere [35]. In particular we can map the sphere into a rectangular domain using spherical coordinates (θ, ϕ); however, to simplify certain formulas we choose corodinates (z, ϕ), where $z = \cos\theta$, so that the differential element of directions becomes $du = \sin\theta\, d\theta\, d\phi = dz\, d\phi$.

Next we show that the value of $K(u)$ for any fixed given value of u can be computed exactly via analytic (nonnumerical) integration.

We compute the value of $K(u)$ for polyhedral domains and polynomial distributions by means of the following algorithm. The key observation is that the values ℓ_1 and ℓ_2 in the expression for $w_B(L)$ are piecewise linear and that $w_B(L)$ is a piecewise-polynomial function.

1. Fix an orthogonal coordinate system (x', y', z'), where the z' axis is parallel to the direction u, and (x', y') span the plane S_u; next, orthogonally project the edges of the polyhedron B over S_u.

2. Compute the transformed $\sigma(x', y', z') \equiv \rho(x, y, z)$ by means of a change of variables; if ρ is a polynomial in (x, y, z), then also σ is a polynomial in (x', y', z'); thus, it is possible to compute symbolically $\overline{\sigma}$, $\overline{\overline{\sigma}}$, and $\int \overline{\sigma}^2$.

3. Compute the partition of the plane induced by the projected edges; to this purpose a variety of algorithms exist in computational geometry literature [36, 37]. The work required at this step is $O((n + k)\log n)$, where n is the number of edges and k is the number of intersections between projected edges, using a method of Bentley and Ottman [38].

4. The global integral $K(u)$ can be obtained by summing the quantities $K_f(u) = \int_{s \in f} w_B(s, u)\, ds$, where f ranges among all the faces of the planar decomposition.

5. For each face f in the planar decomposition, the quantities ℓ_1 and ℓ_2 in (12) are linear functions of x', y'; so their analytic expression can be interpolated from their values at the vertices of f.

6. Since ℓ_1, ℓ_2, and σ are polynomials, the function $w_B(s, u)$ is also a polynomial, whose expression can be computed analytically.

7. Apply Green's theorem to compute the value $K_f(u)$ using only the values of w_B at the vertices of face f.

8. Finally, compute $K(u) = \sum_f K_f(u)$.

The values of ℓ_1, ℓ_2 at the vertices of the planar decomposition can be computed by visiting the graph representing the decomposition. The procedure described above applies when B is a polyhedron and ρ is a polynomial; however, it applies also to any another function for which easy algebraic manipulation is possible. Notice that these two conditions influence two different aspects of the computation: if B is not a polyhedron, but we can compute ℓ_1, ℓ_2 exactly, we can still compute $w_B(L)$ and perform numerical integration over the directions u; on the other hand, if ρ is not easily manipulable, we need numerical integration also to obtain the value $w_B(L)$.

5. RESULTS OF NUMERICAL EXPERIMENTS

In this section we discuss our implementation of the algorithm for the computation of the electrostatic energy of a generic polyhedral object. Then we present numerical experiments, for the case of a homogeneously charged cube and a homogeneously charged parallelepiped. Overall, we tried six different integration methods for the evaluation of the integral (13) and two different implementations of the computation of the kernel (14).

5.1. *Setup of Numerical Experiments*

We first implemented the algorithm that computes $K(u)$ in C++ language. We used the C++ class library LEDA (Library of Efficient Data types and Algorithms) [39], available on the internet at the address `http://www.mpi-sb.mpg.de`. This library contains a routine that computes the planar decomposition induced by a set of segments, using the sweep-type algorithm described in [38].

The numerical experiment consisted in computing expression (10) using different quadrature schemes for integrating over the directions. We tried the following quadrature schemes:

1. Monte Carlo integration. For this scheme, there exist also theoretical results that relate the behaviour of the error to the geometry of the body [40].

2. Quasi-Monte Carlo integration [41]; FORTRAN routines for generating Halton, Sobol, and Faure quasi-random sequences of points were taken from the *Collected Algorithms from ACM* [42]; this package is also available on the internet from a variety of sites (e.g., at the URL `http://www.math.hkbu.edu.hk/qmc`). The experiments were done according to the general framework described in [43];

3. Adaptive multidimensional Gaussian integration; we used routine D01FCF in the NAG library, which is a collection of Fortran routines maintained by the Numerical Algorithms Group [44].

As we will see in the next subsection, the generic implementation, which relies exclusively on standard pieces of software, does not fully exploit the advantages of the new method. In order to obtain better results, we first of all implemented the calculation of the kernel $K(u)$ in C language, using algorithms written on purpose rather than general libraries. Although not highly optimized, this code runs about 40% faster than the previous one.

Moreover, we used a specialized integration algorithm, which is extensively described in [32, 31]. This algorithm adaptively decomposes the integration domain into subdomains over which the function $K(u)$ is well behaved; then it performs a standard Gaussian quadrature over each subdomain, summing all the results in the end.

The idea behind the algorithm is that the function $K(u)$ has continuous derivatives in each region where the projection of the polyhedron over S_u is combinatorically the same. While u varies among all the directions, a combinatorial change happens whenever a vertex is projected on the projection of an edge; this corresponds to a certain great circle in the hemisphere of directions $\frac{1}{2}\Omega$, where $K(u)$ may have discontinuous derivatives.

The algorithm tries all the pairs of vertices and edges (v, e) and identifies the great circle which corresponds to the directions u such that v is projected onto e in S_u. The union of these great circles decomposes the hemisphere $\frac{1}{2}\Omega$ into regions in which the projection of the polyhedron is combinatorically the same. In each such region $K(u)$ is well behaved and the Gaussian quadrature succeeds in obtaining a high convergence rate.

The algorithm with the new integration method (which decomposes the domain and then applies Gaussian integration) and the C code for the kernel $K(u)$ will be denoted with DGQ (decomposing Gaussian quadrature). Note that, denoting with N the number of evaluations of $K(u)$, the relation $N \leftrightarrow$ time depends on the code used for $K(u)$, while the relation $N \leftrightarrow$ accuracy depends on the integration method.

5.2. *Numerical Results*

We performed numerical experiments on the computation of the energy of a cube with unit side length, uniformly charged with density $\rho = 1$. Hummer [26] gives an analytic formula for computing the potential of the cube at any point. Integrating this formula over $[0, 1]^3$ with NAG we were able to obtain a very precise reference value for the energy of a unit cube,

$$E \approx 0.94115632219486 \text{ erg}, \tag{15}$$

with an estimated error of the order of 10^{-14}. (See Table III to examine the convergence of this integration.)

For each of the standard rules of integration discussed in the previous subsection, we carried out 36 different computations, varying the initial rotation of the cube and the seed for the pseudo-random numbers used in the Monte Carlo algorithm. We then computed for each number N of function evaluations the root mean square error, i.e. $\bar{\epsilon}_N = (\sum_j \epsilon_{j,N}^2 / N)^{1/2}$, where $\epsilon_{j,N}$ is the absolute error of the jth run after N function evaluations. Note that, being the value of the integral close to 1, the values $\epsilon_{j,N}$ represent quite well also the relative error.

The results for the Monte Carlo, quasi Monte Carlo, and NAG integration are shown in Table I. The results obtained with the DGQ method are in Table II. There we show for exponentially increasing values of N the value $-\log_{10} \bar{\epsilon}_N$. This number represents the

TABLE I
Energy of Uniformly Charged Cube, Standard Methods

N	Time	Monte Carlo	Halton	Faure	Sobol'	NAG
150	0.82	2.60	2.89	3.03	2.95	2.70
200	1.09	2.72	3.00	3.29	3.09	2.85
300	1.63	2.76	3.27	3.26	3.12	2.92
450	2.43	2.85	3.48	3.54	3.56	3.05
550	2.98	2.91	3.61	3.61	3.59	3.27
750	3.79	2.99	3.60	3.76	3.59	3.42
1050	5.68	3.05	3.87	4.06	3.90	3.62
1450	7.86	3.14	4.14	3.96	3.97	3.67
2050	11.1	3.19	4.06	4.25	4.30	3.76
2950	15.9	3.25	4.25	4.29	4.26	3.84
4100	22.2	3.37	4.26	4.42	4.54	3.86
5800	31.4	3.39	4.48	4.40	4.47	4.58
8200	44.4	3.48	4.69	4.64	4.82	5.04
11600	62.7	3.60	4.76	4.83	4.73	5.35
16400	88.7	3.63	5.09	5.04	5.05	5.61
23200	125	3.70	4.86	5.01	5.08	5.65
32800	177	3.76	5.44	5.40	5.30	6.16
		$\alpha = 0.53$	$\alpha = 1.02$	$\alpha = 1.00$	$\alpha = 1.03$	$\alpha = 1.69$

accuracy of the result, in decimal digits, after N evaluations of $K(u)$. The same results are shown graphically in Fig. 1, in bilogarithmic scale.

All the computations were done on a Pentium II 200MHz computer. In the tables we also show the time in seconds needed for one run to achieve N evaluations of $K(u)$. The value α at the bottom of each column is the convergence rate of the method. It was obtained by a least-square fitting of the values $\overline{\epsilon}_N$, looking for a behaviour like $cN^{-\alpha}$.

In [40] it is shown that the variance of $K(u)$, in the uniform distribution case, is bounded, so we can expect a convergence rate of $1/2$ from the Monte Carlo method. From the results, it is clear that Monte Carlo method performs exactly as expected. Quasi Monte Carlo methods are superior and have a convergence rate very close to the one predicted by theory (error decreases as $\log^2 N/N$ for two-dimensional integration). The different sequences give a very similar behaviour both in error and convergence rate.

TABLE II
Energy of Uniformly Charged Cube, DGQ Method

N	Time	DGQ
256	1.0	3.4
576	2.3	4.4
1024	4.0	5.7
1600	6.3	7.1
2304	9.1	8.6
3136	12	10.0
4096	16	11.0

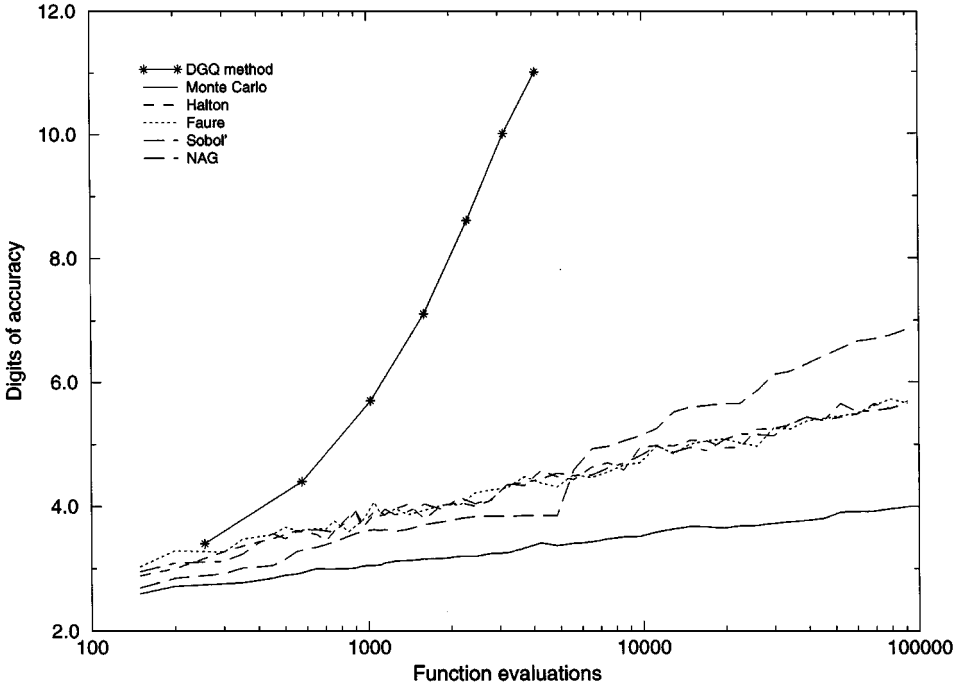

FIG. 1. Energy of the uniformly charged cube.

The results of Monte Carlo methods can be compared to those in Morokoff and Caflisch's work [43]. For a function continuous but not differentiable, defined on a sphere in dimension 2, they exhibit convergence rates between 0.5 (M.C.) and 1.00 (Q.M.C.), with an accuracy of 1.6 digit (M.C.) and 2.85–3.22 digits (Q.M.C.) when $N = 32768$.

The behaviour of the NAG routine is better than that of Monte Carlo method, but the presence of discontinuities in $K(u)$ is a great obstacle in achieving a high convergence rate. Instead, the DGQ method, which prevents discontinuities by subdividing the domain, achieves an error of 10^{-11} in only 16 s. We stress that this method is general and does not use any property of the cube, so we expect a similar behaviour for any object not stretched in one direction.

5.3. *Exploiting Symmetries*

In the integration above we did not take into account the symmetry of the cube when integrating over the directions u. However, in real applications, exploiting the symmetry of the objects involved can save a lot of computations. If we do exploit the symmetry of the cube, we can restrict integration to only $1/24$ of the set $\frac{1}{2}\Omega$ (for example, in the set $\phi \in [0, \pi/4]$, $z \in [(2 + \tan^2 \phi)^{-1/2}, 1]$). In this way we limit the integration in a region where $K(u)$ is well behaved, and we do not waste computations for points which give the same value. Although in a similar way, we exploit symmetry better than the DGQ method does, automatically. Note, however, that in this setting the DGQ method is not applicable.

We carried out numerical experiments in this setting, using the standard integration techniques and the C++ code for $K(u)$. The Monte Carlo method was run with 36 different

TABLE III
Energy of Cube, Exploiting Symmetries

N	Monte Carlo	Halton	Faure	Sobol'	NAG	$\int$ Hummer
150	2.55	3.37	3.37	3.44	6.57	9.56
200	2.62	3.52	3.34	3.50	6.54	9.21
300	2.73	3.81	3.61	3.61	7.87	9.29
400	2.75	3.82	3.85	3.83	7.73	10.03
550	2.87	3.97	3.81	3.98	9.29	10.11
750	2.98	3.97	3.91	3.94	9.63	10.21
1050	3.03	4.10	3.98	4.31	9.75	11.38
1450	3.04	4.29	4.21	4.43	10.15	11.05
2050	3.10	4.67	4.37	4.55	11.03	11.32
2900	3.13	4.67	4.64	4.55	12.34	12.02
4100	3.24	4.95	4.69	4.89	13.65	12.15
5800	3.35	4.97	4.93	4.92		13.03
8200	3.40	5.08	4.94	5.22		13.07
11600	3.49	5.29	5.16	5.19		13.36
16400	3.56	5.22	5.64	5.43		13.84
23200	3.64	5.58	5.58	5.45		14.42
32800	3.78	5.70	5.64	5.62		
	$\alpha = 0.56$	$\alpha = 1.04$	$\alpha = 1.05$	$\alpha = 0.98$	$\alpha = 4.03$	

seeds for the generator; for QMC methods we used, in each run, the successive 10^5 points in the sequence; the NAG routine was run only once, being a completely deterministic algorithm.

The results are shown in Table III. The times of computation are the same as in Table I, although if we use the C code for $K(u)$ we could expect a 40% saving. As a reference, the last column shows the accuracy obtained in the same time of computation when we computed the reference value (15) by 3D adaptive integration of the analytic formula by Hummer.

The analysis shows that the adaptive integrator exploits the new setting, achieving a very high accuracy. An error below 10^{-13} is the minimum attained, approximately in 16 s if we use the C code and even faster than we obtained the reference value. All three QMC algorithms perform slightly better, in terms of digits of accuracy, but the convergence rates are approximately the same. The Monte Carlo method does not seem to gain from the use of symmetry.

5.4. *Another Example: A Parallelepiped*

One can notice that for the cube the integrand function $K(u)$ is very well behaved, in the sense that it does not vary much. In fact, it holds $0.8 \leq 6K(u) \leq 1$ for every direction u. This is not the case for general polyhedra, especially if they are stretched in one direction.

In order to better examine this case, we repeated the same numerical experiments taking a $10 \times 1 \times 1$ parallelepiped (with uniform charge density $\rho = 1$). By adapting the formula in [26] we obtained a reference value of 28.52126794 erg for its energy. Notice that in this case the quotient between the maximum ad the minimum value of $K(u)$ is 100. Table IV, Table V, and Fig. 2 show the results, obtained as before by averaging over 36 different runs of the algorithm. The errors shown are the relative errors.

TABLE IV
Energy of Parallelepiped, Standard Methods

N	Monte Carlo	Halton	Faure	Sobol'	NAG
150	0.77	1.27	1.07	1.14	1.08
200	0.80	1.31	1.27	1.30	1.44
300	0.80	1.39	1.36	1.45	1.63
450	0.92	1.64	1.61	1.61	1.97
550	0.95	1.56	1.64	1.88	2.22
750	1.10	1.87	1.81	1.83	2.87
1050	1.22	1.95	1.95	2.03	3.07
1450	1.23	2.08	2.09	1.99	3.17
2050	1.32	2.20	2.59	2.65	3.20
2950	1.35	2.50	2.38	2.40	3.55
4100	1.43	2.49	2.47	2.71	3.71
5800	1.48	2.61	2.60	2.77	3.80
8200	1.57	2.83	3.01	3.03	3.82
11600	1.65	3.04	2.76	2.89	3.82
16400	1.76	3.18	3.18	3.17	3.82
23200	1.85	3.20	3.10	3.24	5.49
32800	1.93	3.60	3.51	3.63	6.18
	$\alpha = 0.51$	$\alpha = 0.94$	$\alpha = 0.93$	$\alpha = 0.95$	$\alpha = 2.04$

One can see that, as expected, the accuracy is worse than in the case of the cube, even if the asymptotic convergence rates are very similar. Moreover, Monte Carlo and quasi Monte Carlo methods seem more sensitive to the variation of $K(u)$ than the adaptive integrator. In any case, the DGQ method is much faster than all the others.

Notice that in real applications objects stretched as our parallelepiped are rarely present, so one should expect a behaviour somewhere in between the cube and the parallelepiped case.

TABLE V
Energy of Parallelepiped, DGQ Method

N	Time	DGQ
256	1.0	2.00
576	2.3	3.08
1024	4.0	3.63
1600	6.3	3.72
2304	9.1	4.03
3136	12	4.41
4096	16	4.82
5184	20	5.23
6400	25	5.66
7744	30	6.08
9216	36	6.51
10816	42	6.91
12544	49	7.29
14400	57	7.70
16384	65	7.80

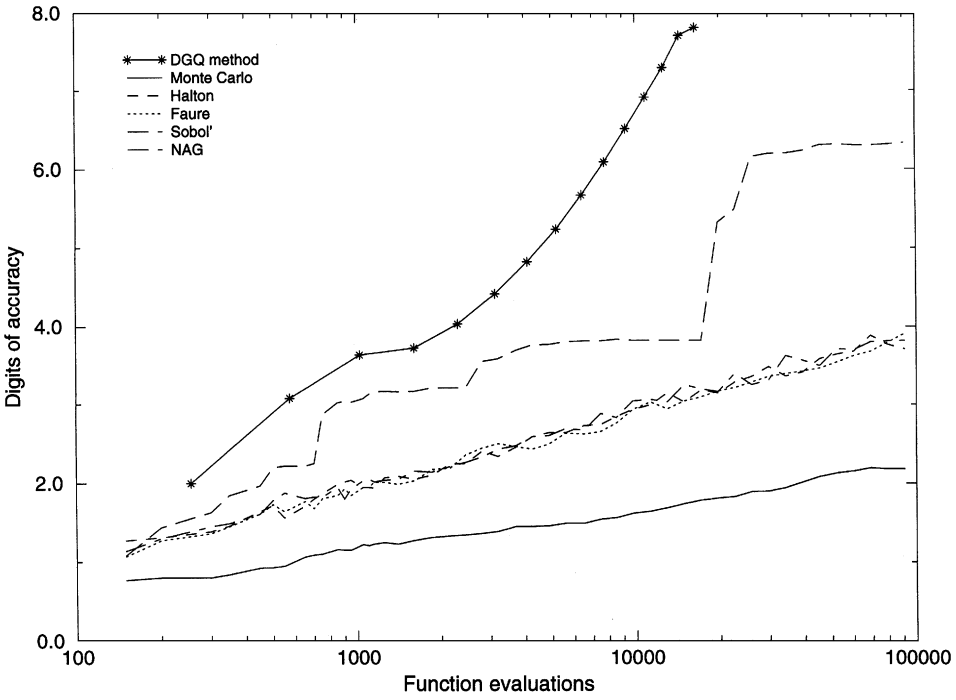

FIG. 2. Energy of the parallelepiped.

6. CONCLUSIONS

In this paper we have shown that six-dimensional integrals defining the Coulomb self-energy of a charge distribution and the mutual energy of two distributions can be reduced to two-dimensional integrals by using integral geometric transformations. This technique is particularly effective for convex polyhedral domains and polynomial distribution of charge, since in this case some auxiliary computation can be done exactly. Preliminary tests on the self-energy of the charged cube, for which reliable reference values are available through an alternative method, show a ratio of precision versus computational effort comparable to those of other methods in literature aimed at three-dimensional integrals.

REFERENCES

1. R. G. Parr and W. Yang, *Density-Functional Theory of Atoms and Molecules* (Oxford Univ. Press, New York, 1989).
2. J. M. Seminario (Ed.), *Recent Developments and Applications of Modern Density Functional Theory* (Elsevier, Amsterdam, 1996).
3. V. R. Saunders, Molecular integrals for Gaussian type functions, in *Methods in Computational Molecular Physics*, edited by H. F. Dieckersen and S. Wilson (Reidel, Dordrecht, 1983), p. 1.
4. S. F. Boys, Electronic wave functions I: A general method of calculation for the stationary states of any molecular system, *Proc. Roy. Soc. Ser. A* **200**, 542 (1950).
5. L. E. McMurchie and E. R. Davidson, One- and two-electron integrals over Cartesian Gaussian functions, *J. Comput. Phys.* **26**, 218 (1978).
6. J. A. Pople and W. J. Hehre, Computation of electron repulsion integrals involving contracted Gaussian basis functions, *J. Comput. Phys.* **27**, 161 (1978).

7. S. Obara and A. Saika, General recurrence formulas for molecular integrals over Cartesian Gaussian functions, *J. Chem. Phys.* **89**, 1540 (1988).
8. J. Rys, M. Dupuis, and H. F. King, Computation of electron repulsion integrals using the Rys quadrature method, *J. Comput. Chem.* **4**, 154 (1983).
9. H. F. King and M. Dupuis, Numerical integration using Rys polynomials, *J. Comput. Phys.* **21**, 144 (1976).
10. J. D. Augspurger, D. E. Bernholdt, and C. E. Dykstra, Concise, open-ended implementation of Rys polynomial evaluation of two-electron integrals, *J. Comput. Chem.* **11**, 972 (1990).
11. P. M. Boerrigter, G. te Velde, and E. J. Baerends, Three-dimensional numerical integration for electronic structure calculations, *Int. J. Quant. Chem.* **33**, 87 (1988).
12. G. te Velde and E. J. Baerends, Numerical integration for polyatomic systems, *J. Comput. Phys.* **99**, 84 (1992).
13. C. B. Haselgrove, A method for numerical integration, *Math. Comp.* **15**, 323 (1961).
14. D. E. Ellis, Application of diphantine integration to Hartree–Fock and configuration interaction calculation, *J. Quant. Chem. Quant. Chem. Sympos.* **2**, 35 (1968).
15. A. D. Becke, A multicenter integration scheme for polyatomic molecules, *J. Chem. Phys.* **88**, 2547 (1988).
16. A. D. Becke and R. M. Dickson, Numerical solution of Poisson's equation in polyatomic molecules, *J. Chem. Phys.* **89**, 2993 (1988).
17. R. M. Dickson and A. D. Becke, Basis-set-free local density functional calculations of geometries of polyatomic molecules, *J. Chem. Phys.* **99**, 3898 (1993).
18. J. M. Perez-Jorda, A. D. Becke, and E. San-Fabian, Automatic numerical integration techniques for polyatomic molecules, *J. Chem. Phys.* **100**, 6520 (1994).
19. C. W. Murray, N. C. Handy, and G. J. Laming, Quadrature schemes for integrals of density functional theory, *Mol. Phys.* **78**, 997 (1993).
20. A. Mayo, The rapid evaluation of integrals of potential theory on general regions, *J. Comput. Phys.* **100**, 236 (1992).
21. A. McKenney, L. Greengard, and A. Mayo, A fast Poisson solver for complex geometries, *J. Comput. Phys.* **118**, 348 (1995).
22. S. G. Brush, H. L. Sahlin, and E. Teller, Monte Carlo study of one component plasma, I *J. Chem. Phys.* **45**(6), 2102 (1966).
23. C. Kittel, *Introduction to Solid State Physics*, 6th ed. (Wiley, New York, 1986).
24. D. J. Adams and G. S. Dubey, Taming the Ewald sum in computer simulations of charged systems, *J. Comput. Phys.* **27**, 156 (1987).
25. B. R. A. Nijboer and Th. W. Ruijgrok, On the energy per particle in three- and two-dimensional Wigner lattices, *J. Statist. Phys.* **53**, 361 (1988).
26. G. Hummer, Electrostatic potential of a homogeneously charged square and cube in two and three dimensions, *J. Electrostatics* **36**, 285 (1996).
27. A. I. Goldman and R. F. Kelton, Quasicrystals and crystalline approximants, *Rev. Modern Phys.* **65**(1), 213 (1993).
28. M. Senechal, Crystals and quasicrystals, in *The CRC Handbook of Discrete and Computational Geometry*, edited by J. E. Goodman and J. O'Rourke (CRC Press, Boca Raton, FL, 1997), p. 933.
29. M. Pellegrini, Monte Carlo approximation of form factors with error bounded a priori, *Discrete Comput. Geom.* **17**, 319 (1997).
30. M. Pellegrini, Electrostatic fields without singularities: Theory and algorithms, in *Proc. 7th ACM-SIAM Symp. on Discrete Algorithms*, 1996, p. 184. [Extended version in Tech. Rep. B4-96-02, Institute for computational Mathematics, Pisa, Italy. Available from `http://www.imc.pi.cnr.it`]
31. M. Pellegrini, *Electrostatic Fields without Singularities: Theory, Algorithms and Error Analysis*, Technical Report B4-97-15, Institute for Computational Mathematics, Pisa, Italy, November 1997. [Available from `http://www.imc.pi.cnr.it`]
32. P. Bientinesi and M. Pellegrini, *Electrostatic Fields without Singularities: Implementation and Experiments*, Technical Report B4-97-16, Institute for Computational Mathematics, Pisa, Italy, November 1997. [Available from `http://www.imc.pi.cnr.it`]
33. V. I. Smirnov, *A Course of Higher Mathematics* (Pergamon, New York, 1964).

34. L. A. Santaló, *Integral Geometry and Geometric Probability, Encyclopedia of Mathematics and Its Applications*, Vol. 1 (Addison-Wesley, Reading, MA, 1976).
35. N. I. Fisher, T. Lewis, and B. J. J. Embleton, *Statistical Analysis of Spherical Data* (Cambridge Univ. Press, Cambridge, 1993).
36. F. P. Preparata and M. I. Shamos, *Computational Geometry: An Introduction* (Springer-Verlag, New York, 1985).
37. K. Mulmuley, *Computational Geometry. An Introduction through Randomized Algorithms* (Prentice–Hall, Englewood Cliffs, NJ, 1994).
38. J. L. Bentley and Th. Ottman, Algorithms for reporting and counting geometric intersections, *IEEE Trans. Comput. C* **28**, 643 (1979).
39. K. Mehlhorn and S. Naher, LEDA: A platform for combinatorial and geometric computing, *Commun. ACM* **38**, 96 (1995).
40. D. Finocchiaro, *Monte Carlo Evaluation of Electrostatic Potential and Potential Energy*, Technical Report B4-96-12, Institute for Computational Mathematics, Pisa, Italy, June 1996. [Available from `http://www.imc.pi.cnr.it`]
41. H. Niederreiter, *Random Number Generation and Quasi-Monte Carlo Methods, CBMS-NSF Regional Conference Series in Appl. Math.* Vol. 63 (SIAM, Philadelphia, 1992).
42. B. L. Fox, Algorithm 647: Implementation and relative efficiency of quasirandom sequence generators, *ACM Trans. Math. Software* **12**(4), 362 (1986).
43. W. J. Morokoff and R. E. Caflish, Quasi-Monte Carlo integration, *J. Comput. Phys.* **122**, 218 (1995).
44. Numerical Algorithms Group, `http://www.nag.co.uk`, `http://www.nag.com`.